Submitted to *Environmental Science and Technology*
January 1986; rev. April 1986.

MATHEMATICAL MODELING OF CHEMICALLY-REACTIVE POLLUTANTS IN INDOOR AIR

William W Nazaroff and Glen R. Cass*
Environmental Engineering Science
California Institute of Technology
Pasadena, CA 91125

Abstract

A general mathematical model is presented for predicting the concentrations of chemically-reactive compounds in indoor air. The model accounts for the effects of ventilation, filtration, heterogeneous removal, direct emission, and photolytic and thermal chemical reactions. The model is applied to the induction of photochemically-reactive pollutants into a museum gallery and the predicted NO, NO_x-NO, and O_3 concentrations are compared to measured data. The model predicts substantial production of several species due to chemical reaction, including HNO_2, HNO_3, NO_3, and N_2O_5. Circumstances in which homogeneous chemistry may assume particular importance are identified and include buildings with glass walls, indoor combustion sources, and direct emission of olefins.

Introduction

Considerable progress has been made recently in developing mathematical models for predicting pollutant concentrations in ambient air. In modeling urban air basins, state-of-the-art approaches utilize a spatially-resolved grid with explicit treatment of advective transport, photochemical reactions, deposition to the earth's surface, and pollutant emissions (1,2). Regional models, used in the study of acid deposition, incorporate many of the above features plus transformation processes involving pollutant reaction within aqueous droplets (3).

By comparison, most approaches to modeling pollutant concentrations in indoor air have been relatively primitive, treating pollutant species as chemically independent, and assuming the building interior to be a single, well-mixed volume (e.g., 4-7). Extended developments have included 1) multichamber formulations (8-10); 2) a model for predicting radon progeny concentrations which incorporated a description of natural convection (11); and 3) explicit treatment of the kinetics of the primary photolytic cycle (9). To date, however, there has not been an indoor air pollution model with the capability of explicitly treating an arbitrary chemical kinetic mechanism.

Despite the moderate success of the models cited above, there are many reasons which argue for development of a model for indoor air pollution that explicitly incorporates reactive chemistry. Data on indoor pollutant concentrations suggest that chemical reactions may proceed at rates comparable to, or even much greater than, the ventilation rate (for example, $NO + O_3$ and $NO_2 + O_3$). A major element of the mass-balance models cited above — the "reactivity" (5) or "indoor sinks" (4) — is not well understood, and there are discrepancies between the wall-loss rates determined in chamber studies and field experiments (12,13). Some secondary pollutants produced, for example, in photochemical smog may not be well-determined by the simple mass-balance approach. And finally, it is becoming increasingly apparent that many indoor environments are as complex in their constitution — if not more so — than polluted outdoor environments (e.g., 14). It is reasonable to expect, given the wide range of pollutants which may be emitted directly indoors, the introduction of pollutants from outdoor air via the ventilation system, and the wide range of indoor lighting levels (and hence photolytic reaction rates), that there are numerous circumstances in which a chemically-explicit model is needed to accurately predict indoor pollutant concentrations.

In this paper, a general mathematical model is formulated that describes the time dependence of indoor air pollutants in a chemically reacting system. An important contribution of this formulation over previous work is the explicit treatment of gas-phase photolytic and thermal reactions. The model is formulated to also compute for each species the production rates associated with ventilation, chemical reaction, and direct emission, and the removal rates associated with ventilation, chemical reaction, filtration and wall loss. As a partial validation of the model, a case is simulated in which outdoor air, containing photochemically reactive air pollutants, is introduced into a museum gallery. The simulated indoor concentrations of ozone, nitric oxide and NO_x-NO are compared with measured data during a two-day period in November 1984. Several interesting perturbations from this base case are considered to study the likely effects of pollutant sources and altered building materials on indoor air chemistry.

Model Formulation

Two fundamental postulates form the basis of the model:

1. The building can be represented as a set of chambers, with the air flow rate from each chamber to all others known as a function of time. Each chamber is visualized as a room or group of rooms. The core of each chamber is considered to be well-mixed and separated from the building surfaces by a thin concentration boundary layer. The details of the boundary layer affect the rate of pollutant removal at fixed surfaces, but may otherwise be neglected in determining pollutant concentrations.

2. Within each chamber, the rate of change of the concentration of each chemical species may be described by an equation of the form

$$\frac{dC}{dt} = S - L\,C \qquad (1)$$

where S represents the sum of all sources: direct emission, advective transport from other chambers (including the mechanical ventilation system and outdoors), and production by chemical reaction; L represents the sum of all sinks: loss by homogeneous chemical reaction, transformation and removal processes occurring on surfaces, and removal by transport from the chamber. S and L are, in general, functions of time and of the concentrations of all pollutant species in all chambers.

The following subsections present details of the manner in which the various elements of the problem are treated in the model.

Ventilation. The treatment of ventilation is an extension of the formulation of Shair and Heitner (4) to incorporate an arbitrary number of chambers. A schematic illustration of the approach is presented in Figure 1. For each chamber, air may enter directly from outside (infiltration), from the mechanical ventilation system (supply), and from each of the other chambers (cross-ventilation). Air may be removed to the outside (exfiltration or exhaust), to the mechanical ventilation system (return), and to each of the other chambers. The mechanical ventilation system is treated as a special chamber having zero volume. In addition to the return air from each chamber, air from outdoors (make-up) may be supplied directly to the mechanical ventilation system. Pollutant removal devices ("filters") may be specified for each return-air line and for the make-up air line. Also, within each chamber, air may be recirculated through a filter. For each pollutant species, the filtration efficiency may be specified by the user.

Mathematically, if we consider a chemically-inert compound, the effects of the ventilation system may be represented as follows:

$$\frac{dC_i}{dt} = \sum_{j=0}^{n} \left[\frac{f_{ji} C_j - f_{ij} C_i}{V_i} \right] + \left[\frac{f_{xi} C_x - f_{ix} C_i}{V_i} \right] - \frac{\eta_{ii} f_{ii} C_i}{V_i} \qquad (2)$$

and

$$C_x = \frac{\sum_{j=0}^{n} \eta_{jx} f_{jx} C_j}{\sum_{j=0}^{n} f_{xj}} \qquad (3)$$

where C_i = the concentration of the compound in chamber i,
V_i = the volume of chamber i,
f_{ij} = the volume flow rate from chamber i to chamber j,
η_{ij} = the efficiency of removal of the compound by the filter located in the air stream connecting chamber i to chamber j, and subscripts x and 0 refer respectively to the mechanical ventilation system and to outdoor air. Equation (2) can readily be converted into the form of equation (1).

Ventilation data for a specific building can be obtained in several ways. Tracer gas experiments may be used to determine flow rates between pairs of chambers (15). Under the uniform-mixing assumption, flow rate measurements in ventilation system ducts may be used to provide the necessary data. In buildings without mechanical ventilation systems, such as many residences, simple models may be used to predict infiltration (16).

Chemical Kinetics. The model can be adapted to incorporate any of the kinetic mechanisms commonly employed in outdoor photochemical air quality models, and can be modified to explicitly treat special problems occuring from the indoor emission of unusual chemical substances. For the examples illustrated in the present paper, a modified version of the Falls and Seinfeld chemical mechanism is employed (1,2,17-20). More than 50 simultaneous chemical reactions are considered. Because the current form of the mechanism is not available in a single reference, it is presented in Table I of this paper.

Photolysis rates. A number of important atmospheric chemical reactions are photolytic in nature. Rates of such reactions depend on the spherically integrated photon flux, and are commonly expressed as

$$k_p = \int_0^\infty \sigma[\lambda]\, \phi[\lambda]\, I[\lambda,t]\ \ d\lambda \qquad (4)$$

where $\sigma[\lambda]$ is the absorption cross-section of the molecule (cm^2), $\phi[\lambda]$ is the quantum yield, $I[\lambda,t]$ is the photon flux density (photons cm^{-3} s^{-1}), and λ is the wavelength of light (cm).

The most accurate calculation of photolysis rates within a given building requires data on the spectral, spatial, and temporal distribution of the ambient lighting, and the model is capable of handling information provided at that level of detail. However, in many cases lighting levels indoors are so much lower than those outdoors that many otherwise important photolytic reactions proceed at small or even negligible rates. For such cases an approximate approach is provided.

In the approximate case, light is treated as having two components, ultraviolet (300 - 400 nm) and visible (400 - 760 nm). Within each component, the spectral distribution is assumed to be flat. Consequently,

$$k_p = h_{uv}\, I_{uv} + h_{vis}\, I_{vis}\ , \qquad (5)$$

$$h_{uv} = (100\ nm)^{-1} \int_{300\ nm}^{400\ nm} \sigma\ \phi\ d\lambda \qquad (6)$$

$$h_{vis} = (360\ nm)^{-1} \int_{400\ nm}^{760\ nm} \sigma\phi\ d\lambda \qquad (7)$$

In equation (5), I_{uv} and I_{vis} represent the spherically integrated (spatially averaged) photon flux (photons $cm^{-2}\ s^{-1}$) in the ultraviolet and visible bands, respectively. The constants h_{uv} and h_{vis} are determined from published data (21,22) and are presented in Table II.

In the model, the ultraviolet and visible fluxes are each assumed to have two components, one due to artificial lighting, the other due to sunlight entering through windows or skylights. For the former, hourly values of the photon flux are specified in each band. For the latter, hourly values of ultraviolet and visible attenuation factors are specified. These factors are then applied to the outdoor photon fluxes determined using a solar simulator (22).

For calculations of outdoor radical concentrations, outdoor photolysis rates are required. Here, the approach of McRae et al. (22) is followed without modification.

Data on indoor light levels sufficient to exercise the model for a specific building may be obtained with a radiometer and ultraviolet light meter (23,24) as described in a later section of this paper. Ultraviolet photon flux also may be inferred by measuring the photolysis rate of NO_2 (25).

Treatment of Highly-Reactive Species. In the indoor model calculations, the pseudo-steady state approximation (PSSA) (26) is applied for O, OH, and RO. The PSSA is also employed to determine the outdoor concentrations of these three species and HNO_4, HO_2, NO_3, N_2O_5, RCO_3, RNO_4, and RO_2 as has been done in simulating outdoor air pollution (27).

Heterogeneous Reactions. In addition to photolytic and thermal reactions occurring in the gas phase, important processes may occur on fixed surfaces such as the floor, walls and ceiling, and on or within airborne particles. Considerable evidence demonstrates that such processes

have substantial impact on both outdoor (e.g., 20) and indoor (e.g., 4) pollutant concentrations.

In previous indoor air pollution models, these processes have been lumped into a first-order decompostion rate, k_s, often assumed to take place entirely on fixed surfaces. An alternative, but nearly equivalent, formulation is in terms of deposition velocity, v_g, which is defined as the ratio of the pollutant flux to a surface to the free-stream concentration. The rate of change of pollutant concentration due to this process alone is then given by

$$\frac{dC}{dt} = - k_s C = - v_g \frac{A}{V} C \qquad (8)$$

where A/V represents the superficial surface-to-volume ratio of the room.

This approach is far from ideal. Processes such as the catalytic conversion of one pollutant species to another and adsorption followed a substantial time later by desorption are not accomodated by this approach. Yet recent evidence suggests that NO_2 may be converted to NO on walls (6), and that, in the presence of NO_2, nitrous acid is formed at substantial rates by heterogeneous reaction (28,29). At present too little is known to incorporate an explicit description of important surface reactions other than unimolecular decomposition and irreversible adsorption.

Measurements of heterogeneous reaction rate or deposition velocity have been reported for several species, as summarized in Table III.

The loss rate depends, in general, on not only the combined reactivity of the compound and the surface, but also on the degree of air movement. Since direct evidence on surface-loss rates of some highly-reactive species in the model do not exist (e.g., for HNO_3), it is appropriate that evidence pertaining to the transport-limited deposition velocity be considered.

Although seldom realized in rooms, the case of perfectly still air represents the lower bound on transport-limited deposition velocity. Here, the deposition velocity is of order 10^{-3} cm s^{-1}, determined by the molecular diffusion coefficient divided by a characteristic dimension of the room.

For rooms in which the air is not still, the analogy between heat and mass transfer can be used to obtain estimates of the transport-limited deposition velocity. Gadgil (30) developed a model to predict the rate of heat transfer from room walls due to natural convection. In simulating a

3 x 3 x 3 m enclosure with one wall maintained at 4.5 deg C higher than the other surfaces, he found an average Nusselt number of 145 for the hot wall. For a compound with a diffusion coefficient of 0.2 $cm^2\ s^{-1}$, the transport-limited deposition velocity to this wall would be 0.1 cm s^{-1}. This compares well to the deposition velocity of 0.13 cm s^{-1}, obtained by applying the Von Karman integral momentum balance to a 3-m long, vertically-oriented plate, heated to 4.5 deg C above the free-stream air (31). Wilson (32) measured the relaxation time for air temperature in a suddenly-cooled room. His results suggest a transport-limited deposition velocity of 0.07 cm s^{-1} for natural convection and 0.18 cm s^{-1} for stirred air, again assuming a diffusion coefficient of 0.2 $cm^2\ s^{-1}$.

Somewhat higher values are indicated by experimental studies of the behavior of unattached decay products of radon in rooms. The deposition velocity for these species, which are believed to be removed at surfaces at the transport-limited rate, have been found to be 0.06 - 0.6 cm s^{-1}, with the consensus value of 0.2 cm s^{-1} (33). The diffusion coefficient of these species is approx. 0.05 $cm^2\ s^{-1}$, smaller than that for gaseous pollutants with lower molecular weights.

The results from Wilson and from the theoretical heat-transfer studies suggest that for circumstances in which room air is not highly stirred, the average transport-limited deposition velocity is within 50% of 0.07 cm s^{-1}. Further research is needed to resolve the discrepancy with studies of radon decay-product removal at surfaces.

Outdoor Concentrations. With the current chemical mechanism, the model requires as input the hourly-averaged outdoor concentration of 15 species or groups of species. These data may be obtained by direct outdoor measurement or from a photochemical air quality model that describes the chemical evolution of the outdoor air over time (1,20). For the application reported in this paper, an approach was used which combines outdoor monitoring data with inferences based on detailed experimental and modeling studies.

Initial Conditions. The initial indoor pollutant concentrations are treated in the same way as the outdoor concentrations: concentrations of fifteen species are specified and the remaining ten are computed assuming that steady-state conditions prevail. For most buildings, simulation results are relatively insensitive to changes in the initial conditions: the limiting characteristic time associated with a perturbed initial condition is given by the inverse air-exchange rate which in many cases is less than an hour.

Direct Emissions. The model accepts as input the direct indoor emission of any species other than O, OH, and RO. As currently formulated, hourly-averaged values are specified, and linear-interpolation is used to obtain the emission rate at any instant during the simulation. This rate is added directly to the source term S in equation (1).

Numerical Solution Technique. The procedure used for solving the system of coupled differential equations that constitutes the model is known as the asymptotic integration method (34). The implementation used in the present model was slightly modified from that established by McRae et al (27). The program is written in Vax-11 Fortran and is run on a Vax-11/750. A 24-hour simulation of a single chamber with an average integration time step of 10 s requires approximately 8 minutes of CPU time.

Model Application: Virginia Steele Scott Gallery

Introduction. Control of indoor pollutants is sought not only to prevent adverse health effects but also to limit the rate of materials damage. Some of the most stringent standards for indoor air quality are specified for museums, archives, and rare book libraries. Since these collections must be preserved indefinitely, even very slow rates of deterioration could lead to unacceptable accumulated damage. Recommended objectives for indoor SO_2, NO_x, and O_3 concentrations in such facilities are a few parts per billion (35). Strong acids (e.g., HCl), organic acids (e.g., acetic acid) and formaldehyde are to be controlled to the lowest possible levels (36).

Analytical tools are needed both to predict the levels of chemically complex mixtures that will occur in new buildings prior to their construction, and to diagnose the source of pollutants present in existing facilities. Surface loss of pollutants is particularly important in museums as it indicates the dose delivered to the collection. In the present paper, simulations are conducted of pollutant levels in a newly constructed museum, based on data taken for this purpose at the Virginia Steele Scott Gallery in San Marino, California. First, the model is exercised to verify that it correctly represents indoor pollutant levels in this building as it was constructed. Next, the effect of a series of hypothetical perturbations on that building's design are analyzed. These cases illustrate circumstances in which homogeneous chemistry in indoor air assumes

added significance in determining the concentrations of photochemically-reactive pollutants.

Description of the Site. Figure 2 shows a floor plan of the gallery and the ventilation flow rates, taken from the architectural plans and engineering specifications. The conditioned volume of the building is 2530 m^3 and the superficial surface area is 3060 m^2. In the gallery areas, rooms 101 and 102, which constitute 86% of the conditioned volume, the floors are oak plank, and the walls are painted plaster and plywood. The ceiling consists of plaster-veneer coffered beams and plastic diffusers. Above room 101 are skylights; fluorescent lamps behind the diffusers provide background lighting to room 102. The lighting in both rooms is supplemented by track lamps. Floor coverings in the other rooms are granite or ceramic tile, or linoleum-type flooring. Walls and ceilings are, for the most part, gypsum dry-wall.

The ventilation system is designed to maintain a temperature of 70±1 °F and a relative humidity of 50±3% in the galleries. The only pollutant removal devices in the ventilation system are strainer mat-type filters (U.L. Class 2, Farr 30/30), designed to remove coarse particulate matter. When the internal recirculation fan is on, the total air flow rate through the mechanical ventilation system is 345 $m^3\ min^{-1}$. The outdoor make-up air flow rate assumes two values: 85 $m^3\ min^{-1}$ during the day and 14 $m^3\ min^{-1}$ at night. The daytime setting was maintained from approximately 7 AM to 6 PM during the study period. In each room, supply and return registers are located on the ceiling raising the possibility of ventilation "short-circuiting" which would lead to a smaller effective ventilation rate than suggested by the flow rate data. However, the relatively low outdoor-air exchange rate (0.3-2.0 h^{-1}) and the absence of rapid fluctuations in monitored pollutant concentrations, combined with the relatively large recirculation rate (8 h^{-1}), suggests that convection was sufficient to effect rapid mixing during the daytime. On the other hand, the indoor data show fluctuations in pollutant concentrations at night that could be due to incomplete mixing.

Monitoring Experiment. For a ten-day period beginning on October 30, 1984, O_3, NO, and NO_2 concentrations were monitored inside and outside the Scott Gallery. Ozone concentrations were measured with a pair of UV photometric ozone monitors (Dasibi models 1003-AH and 1003-PC). A pair of chemiluminescent NO_x monitors (Thermo Electron Corporation, model 14 B/E) was used to measure NO and NO_2. NO_2 values

measured by this method include contributions from other nitrogen-containing species such as HNO_3 and PAN (37). The symbol NO_2* will be used to signify measurement data for this group of species, determined as NO_x-NO by the monitors. The NO_x monitors were calibrated daily against zero air and a known supply of 0.4 ppm NO in nitrogen. Data from all instruments were continuously registered on strip-chart recorders. Pollutant concentration values averaged over twelve-minute intervals throughout the experiment were extracted from the strip-chart records.

On two days during the monitoring period, November 4 and 5, peak outdoor O_3 concentrations exceeded 120 ppb in the presence of NO_x levels in excess of 200 ppb. Because of the relatively high pollution levels, model validation efforts were focused on these days.

Input Data for the Validation. Because of the large recirculation rate and the large fractional volume in room 101, the Scott Gallery was initially modeled as a single chamber. Ventilation rates were those indicated in the architectural specifications, as the building had been balanced recently against those specifications. Filter efficiency was assumed to be zero for all gaseous species.

Ultraviolet and visible photon fluxes were computed from data taken both in room 101 and outdoors with a radiometer equipped with a UV cutoff filter (Eppley model PSP; filter GG 395) and a spot meter (UVC meter) designed to measure the ratio of radiance in the ultraviolet to the total illuminance (23,24). From these measurements the skylights were estimated to transfer a photon flux equal to 0.7% of the visible light and 0.15% of the ultraviolet light falling on the roof of the building outdoors. Artificial lighting was estimated to contribute flux densities of 0.7×10^{15} and 2.3×10^{13} photons cm^{-2} s^{-1} in the visible and ultraviolet, respectively, between 9 AM and 6 PM.

For the "base case" simulation, deposition velocities reported in the literature for NO, NO_2, O_3, and HCHO have been used (see Table IV). Higher aldehydes were assumed to have the same surface removal characteristics as formaldehyde. Removal of highly reactive species (H_2O_2, PAN, HNO_2, RNO_2, RNO_4, HNO_3, N_2O_5, NO_3, HO_2, RO_2, HNO_4, and RCO_3) was taken to proceed at a transport-limited rate, based principally on Wilson's experiments. Other species (e.g., CO) are assumed to be sufficiently inert that their removal rates at building surfaces are negligible.

Data on outdoor concentrations of the fifteen pollutants required by the model were specified by the following approach.

The outdoor monitoring data on O_3, NO, and NO_2* collected on-site were used. Based on the results of monitoring studies (38,39), outdoor HNO_3 and PAN concentrations in ppb were estimated as 10% and 5%, respectively, of the outdoor ozone concentration in ppb. The concentrations of HNO_3 and PAN were subtracted from the measured NO_x-NO concentration to correct for interference in determining the NO_2 values used in the validation study (37).

The outdoor data taken at the Scott Gallery were compared with NO, NO_x-NO, and O_3 measurements reported for the same time interval by the South Coast Air Quality Management District's (SCAQMD) monitoring station in Pasadena, located within 1.5 km of the Scott Gallery. Good agreement between these two data sets was found. Having established the close correspondence between these two monitoring sites, data for CO from the Pasadena station of the SCAQMD were used.

Hourly data on total hydrocarbons are measured by the SCAQMD at Azusa, California. These total hydrocarbon data were subdivided into formaldehyde, higher aldehydes, olefins, alkanes, aromatics and ethylene using the splitting factors determined by Russell and Cass (40) based on detailed analysis of the composition of morning air in Los Angeles reported by Grosjean and Fung (41).

Input data for concentrations of the remaining species in outdoor air (H_2O_2, HNO_2, and RNO_2) were determined from general experience in modeling ambient air pollution in the Los Angeles basin (42). The hydrogen peroxide concentration was assumed to be 5% of the outdoor ozone concentration. Nitrous acid concentration was assumed to peak at 1.5 ppb during the hour after sunrise, falling to zero linearly over an hour on either side of the peak. The outdoor concentration of RNO_2 was assumed to be zero.

The initial indoor concentrations of NO, NO_2 and O_3 were specified based on values measured inside the Scott Gallery. For all other species, the initial concentration was computed by bringing the model to its steady state value based on the initial outdoor concentration, the air-exchange rate, the wall loss rate, and assuming no homogeneous chemical reaction. Since there are no known direct emissions of pollutants within the Scott gallery, indoor pollutant source strengths were set to zero for the base case model calculations.

Perturbations of the Model Parameters. Six simulations in addition to the base case were run to examine the response of the model

to changes in some of the input parameters (see Table IV). Three of these cases were run to examine the sensitivity of the results to assumptions about the input data. In particular, the "low NO_2 wall loss" case was run because indoor and outdoor monitoring data showed that the average total NO_x levels inside the Scott Gallery were very close to those outside. The case with "no explicit chemistry" was run to compare the predictions of previous model formulations with the present work. The "multichamber" case addresses the magnitude of errors resulting from assuming that this building may be represented as a single well-mixed chamber.

The three remaining cases were selected to examine how changes in building design or operation could influence indoor pollutant concentrations through chemical reaction. The case with an "indoor hydrocarbon source" could represent a situation in which fumes from an underground parking garage enter the building, or a case in which solvents are used within the building. The "indoor oxides of nitrogen source" considers the effect of operating combustion appliances. The "glass-walled building" case considers the effects of increased photolytic reaction rates and reduced wall loss rates associated with glass.

Results. A comparison of measured and simulated ozone concentrations is presented in Figure 3. Model results are shown for both the base case and the no-chemistry case. The full kinetic model is slightly better in predicting indoor ozone concentrations, particularly during the morning hours when the presence of a significant nitric oxide concentration constitutes a substantial sink for ozone by reaction 3. As indicated in Table V, the heterogeneous wall loss rate is the dominant factor in accounting for the difference between indoor and outdoor ozone concentrations within this particular building. Chemical reaction is, however, a significant net sink.

Comparisons between measurements and simulations for oxides of nitrogen are presented in Figure 4. At most times the measured NO_x and NO_2* concentrations are seen to lie between the results for the base case and "low NO_2 wall loss" simulations. The nitric oxide concentration, on the other hand, is underpredicted at most times by both simulations, supporting Yamanaka's inference that NO_2 is converted to NO at indoor surfaces (6). The "low NO_2 wall loss" case predicts a total NO_x concentration that is closer to the measured value (5% high) than is the result for the base case simulation (14% low).

Tables V and VI summarize the simulation results, giving average source and sink rates and average concentrations, respectively. Figure 5 presents average concentrations for selected species. Several of the findings are noteworthy.

Comparing the average concentrations for the base case and no chemistry simulations, we see that several nitrogen-containing species—HNO_2, HNO_3, HNO_4, NO_3 and N_2O_5—are produced at substantial net rates by chemical reaction indoors. For the latter two species, indoor concentrations exceed those outdoors. In a conventionally-lit building, formation of these species may occur indoors during the day by reaction pathways normally associated with nighttime chemistry outdoors (20). N_2O_5 recently has been implicated in the production of mutagenic compounds in outdoor air (43); the possibility that N_2O_5 is present at elevated levels indoors should be further studied.

Pitts et al. (28) experimentally demonstrated the production of nitrous acid in an indoor environment with elevated levels of NO_2, and inferred from their data a steady-state average ratio of HNO_2 to NO_2 of 15 x 10^{-3}. The base case indoor simulation also indicates that HNO_2 is formed indoors, but the HNO_2 to NO_2 ratio due to homogeneous gas-phase chemistry alone is lower, 0.4 x 10^{-3}. This discrepancy supports the hypothesis that heterogeneous reactions (e.g., on building surfaces) may play an important role in nitrous acid production.

Information on the flux of reactive species to interior surfaces may be useful in assessing the potential for damage to materials displayed in museums. Under the assumptions of the base case simulation, the average fluxes of O_3 and HNO_3 to the walls during this two-day period were 38.4 and 8.8 mg m^{-2} h^{-1}, respectively.

The results of the multichamber simulation indicate that the treatment of this building as a single chamber is a reasonable approximation. Concentration variations among chambers are approximately 10% or less, due to the relatively high rate of recirculation through the mechanical ventilation system.

The two cases for which an indoor pollutant source is postulated show that such sources may either increase or decrease the concentration of species not directly emitted. For example, the hydrocarbon source leads to substantial reduction in the indoor concentration of O_3 and NO, but markedly increased concentrations of HNO_2, HNO_4, HCHO, and H_2O_2, among

others. The indoor combustion source likewise leads to a consumption of O_3, but increased production of HNO_2, and HNO_3.

In the case of the glass-walled building, indoor concentrations of several key species—including O_3, HNO_2, HNO_3, PAN, and H_2O_2—are increased markedly over the base case values, and in fact are seen to exceed the outdoor levels. In this case, homogeneous chemical reactions are greatly enhanced by the combined effects of increased lighting, leading to higher photolysis rates, and reduced wall loss, leading to higher concentrations of reactive species.

Discussion

The results of this study indicate the importance of homogeneous chemistry as a pollutant transformation process in indoor atmospheres. Concentrations of many species (e.g. O_3) are significantly perturbed by chemical reaction, especially when outdoor air pollutants are combined with direct indoor emissions. For other species (e.g. N_2O_5) an accounting of the effect of homogeneous chemical reactions is essential because the rates of chemical production in indoor air dominate other source terms.

The results of the present work—the reasonable agreement between measured and simulated pollutant concentrations, and the minor effect of treating the Scott Gallery as a four-chamber rather than a one-chamber building—indicate that the assumption that each chamber in the model is well-mixed did not interfere with obtaining accurate results. Additional work to relax the uniform mixing hypothesis is warranted. Efforts to determine the rates of mixing in indoor air and to examine the effect of poor mixing on the apparent rates of chemical reaction are recommended. One approach to relaxing the uniform-mixing assumption is to use the atmospheric diffusion equation (26) in place of equation (1) to describe the time-rate-of-change of pollutant concentrations. To solve the problem using this approach, one requires information on localized indoor air velocities and eddy diffusivities. The basis for describing indoor air motion is partially established in numerical codes for natural convection in enclosures (30). A model that employs an explicit description of air motion at scales smaller than the dimension of the rooms would be considerably more difficult to validate and costly to apply than the present approach. Nevertheless, it could prove quite useful in examining the validity of the uniformly-mixed model, and in treating the mass-transport aspects of surface reaction on a more fundamental basis.

The present model is also restricted in the scope of the transformation processes considered. The explicit description is limited to gaseous pollutants and gas-phase chemistry. The approach taken to account for pollutant interactions at fixed surfaces is a simplified one and possible interactions of gaseous pollutants with suspended particulate matter are not considered at all. The results reported here indicate that a dominant route for removal of highly-reactive pollutants is deposition on walls (see Table V). Also, as discussed above, there are indications that nitrogen-containing species may be chemically transformed rather than simply removed at surfaces. Further research is needed to improve the understanding of these heterogeneous processes. Such work should include carefully-designed experiments that account for both mass transport and surface-reaction kinetics.

The model as presently formulated has a number of important applications in addition to those discussed in this paper. It may be used to assess the effects of filtration of selected compounds, to design indoor air quality control strategies based on ventilation scheduling, and to simulate specialized cases where unusual chemicals are present in an industrial setting. The model is formulated to be a general tool for studying chemically-reactive air pollution systems. Within limits, one can specify an arbitrary chemical mechanism, modify the computer code in a straightforward manner, and simulate an indoor environment in which homogeneous chemical reactions play an important role in determining pollutant concentrations.

Acknowledgments

Discussions with Dr. A.G. Russell provided insight on several aspects of the related problem of modeling outdoor air quality. The research was supported by a contract with the Getty Conservation Institute and by an Earle C. Anthony Graduate Fellowship.

Literature Cited

(1) McRae, G.J.; Goodin, W.R.; Seinfeld, J.H. Atmos. Environ. 1982, 16, 679-696.

(2) McRae, G.J.; Seinfeld, J.H. Atmos. Environ. 1983, 17, 501-522.

(3) Ruff, R.E.; Nitz, K.C.; Ludwig, F.L.; Bhumralkar, C.M.; Shannon, J.D.; Sheih, C.M.; Lee, I.Y.; Kumar, R.; McNaughton, D.J. Atmos. Environ. 1985, 19, 1103-1115.

(4) Shair, F.H.; Heitner, K.L. Environ. Sci. Technol. 1974, 8, 444-451.

(5) Traynor, G.W.; Anthon, D.W.; Hollowell, C.D. Atmos. Environ. 1982, 16, 2979-2987.

(6) Yamanaka, S. Environ. Sci. Technol. 1984, 18, 566-570.

(7) Fisk, W.J. In "Indoor Air: Buildings Ventilation and Thermal Climate"; Berglund, B.; Lindvall, T.; Sundell, J., Eds.; Swedish Council for Building Research: Stockholm, 1984; Vol. 5, pp. 187-192.

(8) Hernandez, T.L.; Ring, J.W. Environ. Int. 1982, 8, 45-57.

(9) Özkaynak, H.; Ryan, P.B.; Allen, G.A.; Turner, W.A. Environ. Int. 1982, 8, 461-471.

(10) Davidson, C.I.; Osborn, J.F.; Fortmann, R.C. In "Indoor Air: Chemical Characterization and Personal Exposure"; Berglund, B.; Lindvall, T.; Sundell, J., Eds.; Swedish Council for Building Research: Stockholm, 1984; Vol. 4, pp. 69-74.

(11) Schiller, G.E. Ph.D. Thesis, University of California, Berkeley, 1984.

(12) Sabersky, R.H.; Sinema, D.A.; Shair, F.H. Environ. Sci. Technol. 1973, 7, 347-353.

(13) Shair, F.H. ASHRAE Trans. 1981, 87 (Part I), 116-139.

(14) Berglund, B.; Linvdall, T.; Sundell, J., Eds. "Indoor Air", Swedish Council for Building Research: Stockholm, 1984; 5 vol.

(15) Sinden, F.W. Building and Environ. 1978, 13, 21-28.

(16) Sherman, M.H. Ph.D. Thesis, University of California, Berkeley, 1980.

(17) Hecht, T.A.; Seinfeld, J.H. Environ. Sci. Technol. 1972, 6, 47-57.

(18) Hecht, T.A.; Seinfeld, J.H.; Dodge, M.C. Environ. Sci. Technol. 1974, 8, 327-339.

(19) Falls, A.H.; Seinfeld, J.H. Environ. Sci. Technol. 1978, 12, 1398-1406.

(20) Russell, A.G.; McRae, G.J.; Cass, G.R. Atmos. Environ. 1985, 19, 893-903.

(21) Baulch, D.L.; Cox, R.A.; Crutzen, P.J.; Hampson, R.F., Jr.; Kerr, J.A.; Troe, J.; Watson, R.T. J. Phys. Chem. Ref. Data, 1982, 11, 327-496.

(22) McRae, G.J. Ph.D. Thesis, California Institute of Technology, Pasadena, 1982.

(23) Hall, E.T. In "London Conference on Museum Climatology"; International Institute for Conservation, London, 1967, pp 151-157.

(24) Thomson, G. In "London Conference on Museum Climatology"; International Institute for Conservation, London, 1967.

(25) Jackson, J.O.; Stedman, D.H.; Smith, R.G.; Hecker, L.H.; Warner, P.O. Rev. Sci. Instrum. 1975, 46, 376-378.

(26) Seinfeld, J.H. "Atmospheric Chemistry and Physics of Air Pollution," J.Wiley and Sons: New York, 1985.

(27) McRae, G.J.; Goodin, W.R.; Seinfeld, J.H. J. Comp. Phys. 1982, 45, 1-42.

(28) Pitts, J.N., Jr.; Wallington, T.J.; Biermann, H.W.; Winer, A.M. Atmos. Environ. 1985, 19, 763-767.

(29) Besemer, A.C.; Nieboer, H. Atmos. Environ. 1985, 19, 507-513.

(30) Gadgil, A. J. Ph.D. Thesis, University of California, Berkeley, 1980.

(31) Eckert, E.R.G.; Drake, R.M., Jr. "Analysis of Heat and Mass Transfer," McGraw-Hill: New York, 1972; p. 528.

(32) Wilson, M.J.G. Proc. Roy. Soc. (London) 1968, A 307, 215-221.

(33) Knutson, E.O. In "Radon and Its Progeny in Indoor Air"; Nazaroff, W.W.; Nero, A.V., Eds.; CRC Press: Boca Raton, Florida, (draft).

(34) Young, T.R.; Boris, J.P. J. Phys. Chem. 1977, 81, 2424-2427.

(35) Baer, N.S.; Banks, P.N. Int. J. of Museum Management and Curatorship 1985, 4, 9-20.

(36) Mathey, R.G.; Faison, T.K.; Silberstein, S.; Woods, J.E.; Johnson, W.B.; Lull, W.P.; Madson, C.A.; Turk, A.; Westlin, K.L.; Banks, P.N. "Air

Quality Criteria for Storage of Paper-Based Archival Records," National Bureau of Standards: Washington, D.C.,1983, NBSIR 83-2795.

(37) Winer, A.M.; Peters, J.W.; Smith, J.P.; Pitts, J.N.,Jr. Environ. Sci. Technol. 1974, 8, 1118-1121.

(38) Hanst, P.L.; Wong, N.W.; Bragin, J. Atmos. Environ. 1982, 16, 969-981.

(39) Tuazon, E.C.; Winer, A.M.; Pitts, J.N., Jr. Environ. Sci. Technol. 1981, 15, 1232-1237.

(40) Russell, A.G.; Cass, G.R. Atmos. Environ. 1986 (in press).

(41) Grosjean, D.; Fung, K. J. Air Pollut. Contr. Ass. 1984, 34, 537-543.

(42) Russell, A.G., Carnegie-Mellon University, personal communication, 1985.

(43) Pitts, J.N., Jr.; Sweetman, J.A.; Zielinska, B.; Atkinson, R.; Winer, A.M.; Harger, W.P. Environ. Sci. Technol. 1985, 19, 1115-1121.

(44) Mueller, F.X.; Loeb, L.; Mapes, W.H. Environ. Sci. Technol. 1973, 7, 342-346.

(45) Sutton, D.J.; Nodolf, K.M.; Makino, K.K. ASHRAE J. 1976 18(9), 21-26.

(46) Traynor, G.W.; Apte, M.G.; Dillworth, J.F.; Hollowell, C.D.; Sterling, E.M. Environ. Int. 1982, 8, 447-452.

(47) Wade, W.A., III; Cote, W.A.; Yocum, J.E. J. Air Pollut. Contr. Ass. 1975, 25, 933-939.

(48) Miyazaki, T. In "Indoor Air: Chemical Characterization and Personal Exposure"; Berglund, B.; Lindvall, T.; Sundell, J., Eds.; Swedish Council for Building Research: Stockholm, 1984; Vol. 4, pp. 103-110.

(49) Revzan, K.L. In "Indoor Air: Building Ventilation and Thermal Climate"; Berglund, B.; Lindvall, T.; Sundell, J., Eds.; Swedish Council for Building Research: Stockholm, 1984; Vol. 5, pp. 65-72.

(50) Summer, W. "Ultraviolet and Infra-Red Engineering," Interscience Publishers: New York, 1962; p. 60.

Table I. Kinetic Mechanism (1,2,20-22)

	Reaction	Rate Constant (ppm min K units)
1	$NO_2 + h\nu \rightarrow NO + O(^3P)$	a
2	$O(^3P) + O_2 + M \rightarrow O_3 + M$	$0.346\ T^{-2}\ exp(510/T)$
3	$O_3 + NO \rightarrow NO_2 + O_2$	$9.245 \times 10^5\ T^{-1}\ exp(-1450/T)$
4	$NO_2 + O(^3P) \rightarrow NO + O_2$	$3.99 \times 10^6\ T^{-1}$
5	$NO + O(^3P) \rightarrow NO_2$	$1.67 \times 10^5\ T^{-1}\ exp(584/T)$
6	$NO_2 + O(^3P) \rightarrow NO_3$	$8.81 \times 10^5\ T^{-1}$
7	$O_3 + NO_2 \rightarrow NO_3 + O_2$	$5.19 \times 10^4\ T^{-1}\ exp(-2450/T)$
8	$NO_3 + NO \rightarrow 2\ NO_2$	$8.81 \times 10^6\ T^{-1}$
9	$NO + OH \rightarrow HNO_2$	$5.07 \times 10^6\ T^{-1}$
10	$HNO_2 + h\nu \rightarrow NO + OH$	a
11	$HO_2 + NO_2 \rightarrow HNO_2 + O_2$	$17.3\ T^{-1}\ exp(1006/T)$
12	$HNO_2 + OH \rightarrow H_2O + NO_2$	$2.91 \times 10^6\ T^{-1}$
13	$NO_2 + HO_2 \rightarrow HNO_4$	$1.73 \times 10^4\ T^{-1}\ exp(1006/T)$
14	$HNO_4 \rightarrow HO_2 + NO_2$	$1.80 \times 10^{15}\ exp(-9950/T)$
15	$HO_2 + NO \rightarrow NO_2 + OH$	$3.58 \times 10^6\ T^{-1}$
16	$RO_2 + NO \rightarrow NO_2 + RO$	$3.58 \times 10^6\ T^{-1}$
17	$RCO_3 + NO \rightarrow NO_2 + RO_2 + CO_2$	$1.13 \times 10^6\ T^{-1}$
18	$NO_2 + OH \rightarrow HNO_3$	$4.401 \times 10^{17}\ T^{-1}\ (280/T)^{½}\ 10^{(11.6T/(17.4+T))}$
19	$CO + OH\ (+ O_2) \rightarrow HO_2 + CO_2$	$1.31 \times 10^5\ T^{-1}$
20	$O_3 + h\nu \rightarrow O(^3P) + O_2$	a
21	$HCHO + h\nu\ (+ 2\ O_2) \rightarrow 2\ HO_2 + CO$	a
22	$HCHO + h\nu \rightarrow H_2 + CO$	a
23	$HCHO + OH\ (+ O_2) \rightarrow HO_2 + H_2O + CO$	13890
24	$RCHO + h\nu \rightarrow HO_2 + RO_2 + CO$	a
25	$RCHO + OH\ (+ O_2) \rightarrow RCO_3 + H_2O$	25680
26	$C_2H_4 + OH \rightarrow RO_2$	11660
27	$C_2H_4 + O(^3P) \rightarrow HO_2 + RO_2$	1219
28	$OLE + OH \rightarrow RO_2$	89142
29	$OLE + O(^3P) \rightarrow RO_2 + RCO_3$	22118
30	$OLE + O_3 \rightarrow 0.5\ RCHO + 0.5\ HCHO + 0.3\ HO_2 + 0.31\ RO_2 + 0.14\ OH + 0.03\ RO$	0.136
31	$ALK + OH \rightarrow RO_2$	4700
32	$ALK + O(^3P) \rightarrow RO_2 + OH$	99.8
33	$ARO + OH \rightarrow RO_2 + RCHO$	16112
34	$RO \rightarrow HO_2 + 0.5\ HCHO + RCHO$	2.0×10^5
35	$RONO + h\nu \rightarrow RO + NO$	a
36	$RO + NO \rightarrow RONO$	$4.38 \times 10^6\ T^{-1}$
37	$RO + NO_2 \rightarrow RNO_3$	$2.19 \times 10^6\ T^{-1}$

Table I. (Cont.)

	Reaction	Rate Constant (ppm min K units)
38	$RO + NO_2 \rightarrow RCHO + HNO_2$	$1.91 \times 10^5\ T^{-1}$
39	$NO_2 + RO_2 \rightarrow RNO_4$	$1.64 \times 10^6\ T^{-1}$
40[b]		
41	$RNO_4 \rightarrow NO_2 + RO_2$	$1.80 \times 10^{15} \exp(-9950/T)$
42	$RCO_3 + NO_2 \rightarrow PAN$	$6.17 \times 10^5\ T^{-1}$
43	$PAN \rightarrow RCO_3 + NO_2$	$4.77 \times 10^{16} \exp(-12516/T)$
44	$NO_2 + NO_3 \rightarrow N_2O_5$	$7.48 \times 10^5\ T^{-1}$
45	$N_2O_5 \rightarrow NO_2 + NO_3$	$4.07 \times 10^{16} \exp(-11080/T)$
46	$H_2O + N_2O_5 \rightarrow 2\ HNO_3$	$5.66 \times 10^{-4}\ T^{-1}$
47	$O_3 + OH \rightarrow HO_2 + O_2$	$6.62 \times 10^5\ T^{-1} \exp(-1000/T)$
48	$O_3 + HO_2 \rightarrow OH + 2\ O_2$	$4.85 \times 10^3\ T^{-1} \exp(-580/T)$
49	$NO_3 + h\nu \rightarrow NO + O_2$	a
50	$HO_2 + HO_2 \rightarrow H_2O_2 + O_2$	$3.4 \times 10^4\ T^{-1} \exp(1100/T) + 5.8 \times 10^{-5}\ T^{-2} \exp(5800/T)\ [H_2O]$[c]
51	$H_2O_2 + h\nu \rightarrow 2\ OH$	a
52	$RO_2 + RO_2 \rightarrow 2\ RO + O_2$	$2.04 \times 10^4\ T^{-1} \exp(223/T)$
53	$NO_3 + HCHO\ (+ O_2) \rightarrow HNO_3 + HO_2 + CO$	0.86
54	$NO_3 + RCHO\ (+ O_2) \rightarrow HNO_3 + RCO_3$	3.6
55	$NO_3 + h\nu \rightarrow NO_2 + O(^3P)$	a
56	$NO_3 + OLE \rightarrow RPN$[d]	$3288\ T^{-1}$
57	$NO_2 + NO_3 \rightarrow NO_2 + NO + O_2$	$175\ T^{-1}$

[a] Rate depends on photon flux; see Table II.

[b] Reaction in earlier mechanisms that was subsequently eliminated.

[c] $[H_2O]$ is water vapor concentration in ppm.

[d] Nitroxyperoxyalkyl nitrates and dinitrates, not considered to participate in further chemistry.

Table II. Coefficients Used to Determine Photolysis Rates (21,22)

Reaction		h_{uv} (10^{-20} cm^2)	h_{vis} (10^{-20} cm^2)
1	$NO_2 + h\nu \rightarrow NO + O(^3P)$	39.4	0.95
10	$HNO_2 + h\nu \rightarrow NO + OH$	8.1	0
20	$O_3 + h\nu \rightarrow O(^3P) + O_2$	0.16	0.21
21	$HCHO + h\nu (+ 2\ O_2) \rightarrow 2\ HO_2 + CO$	0.58	0
22	$HCHO + h\nu \rightarrow H_2 + CO$	0.43	0
24	$RCHO + h\nu \rightarrow HO_2 + RO_2 + CO$	0.56	0
35	$RONO + h\nu \rightarrow RO + NO$	8.7	0.21
49	$NO_3 + h\nu \rightarrow NO + O_2$	0	11.5
51	$H_2O_2 + h\nu \rightarrow 2\ OH$	0.13	0
55	$NO_3 + h\nu \rightarrow NO_2 + O(^3P)$	0	99.1

Table III. Measurements of Indoor Deposition Velocity

Species	Dep. Vel. (cm s^{-1})	Notes
O_3	0.036 ± 0.021	24 measurements in 13 buildings; one excluded due to suspected NO source (4).
	0.02 - 0.07	inferred from measurements of ozone loss rate in a single residence (12).
	0.001 - 0.11 (New) 0.0005 - 0.015 (Aged)	for various materials exposed in a chamber study (12).
	0.027[a] (Aluminum) 0.015 (Stainless Steel) 0.036 (Office) 0.061 (Bedroom)	inferred from measurements of ozone loss rate in experimental chambers and rooms (44).
	0.001 - 0.20	for various typical indoor materials exposed in a test room (45).
NO	-0.0001 ± 0.001	decay rate in a house of emissions from gas-fired range; assumed A/V = 2 m^{-1} (46).
	0.0008	decay rate in a house of emissions from gas-fired range; assumed A/V = 2 m^{-1} (47).
	0.0017 ± 0.0014	analysis of data from gas-stove emissions experiment using simplified kinetic model; assumed A/V = 2 m^{-1} (9).
	0.0000 - 0.003	for various indoor surface materials, measured in test chamber; 20-26 C, 40-60% RH (48).
NO_2	0.018 ± 0.009	concentration decay rate from gas-stove emission experiment in test room; 11 runs; includes homogeneous reactions; assumed A/V = 2 m^{-1} (5).
	0.011	decay rate in a house of emissions from gas-fired range; assumed A/V = 2 m^{-1} (47).
	0.006 (50% RH) 0.011 (60% RH) 0.017 (70% RH)	analysis of decay rates from emissions due to gas- and kerosene-fired unvented heaters; attempt to exclude homogeneous reactions (6).
	0.0003 - 0.12	for various indoor surface materials, measured in test chamber; 20-26 C, 40-60% RH (48).
HCHO	0.005 ± 0.003	analysis of concentration decay rate from gas-stove emission experiment in test room; 5 runs; includes homogeneous reactions; assumed A/V = 2 m^{-1} (5).

[a] Data show strong positive correlation with relative humidity, varying from 0.0007 cm/s at 5% RH to 0.028 cm/s at 87% RH

Table IV. Simulation Input Parameters

Base Case

Deposition Vel.(cm s^{-1}):	O3	0.036
	NO2	0.006
	HCHO,RCHO	0.005
	PAN	0.035
	HNO2, HNO3, HNO4, HO2, H2O2, NO3, N2O5, RCO3, RNO4, RONO, RO2	0.07
	NO, ALK, ARO, CO, C2H4, OLE	0.0

All other input parameters discussed in text.

Low NO2 Wall Loss (WL)

Same as base case except deposition velocity for NO2 changed to 0.0.

No Explicit Chemistry (No Chem)

Same as base case except rates of all reactions in kinetic mechanism set to 0.0.

Multichamber Case

Same as base case except building treated as four chambers:

Chamber 1 - Rooms 101, 101E, 101W, 101N, 101S
Chamber 2 - Room 102
Chamber 3 - Rooms 104, 104A, 105, 105A, 106, 107, 108, 109
Chamber 4 - Rooms 110, 111

Mechanical ventilation rates determined from architectural specifications (see Figure 2). Cross-ventilation flow rates taken as minimum necessary to balance air flows. Artificial lighting assumed same for each chamber. Daylighting only in chamber 1.

Indoor Hydrocarbon Source (HC Source)

Same as base case with added continuous indoor emission of hydrocarbons at following rates (ppb min^{-1}):

Alkanes	46.7
Aromatics	9.6
Olefins	9.6

This corresponds approximately to evaporation of 10 cm^3 hr^{-1} of gasoline (22) and is taken as a model either of the use of a naptha-based solvent as may occur in a preservation lab, or of the presence of an underground garage.

Indoor Oxides of Nitrogen Source (NOx Source)

Same as base case with added emission of combustion-generated pollutants during the hours 0700-1300 at following rates (ppb min^{-1})

Nitrogen dioxide	2.5
Nitric oxide	2.5
Carbon monoxide	64.4
Formaldehyde	0.6

Simulates the emissions due to gas-fired cooking equipment such as might be present in a cafeteria. Emissions data from Traynor et al (5). Assumes 10 range-top burners and 5 ovens (residential sized) on continuously during 6-hour cooking period. Range hoods assumed to reduce emissions into the main volume to 40% of the total (49).

Glass-Walled Building (Glass-Walled)

Changes from base case: 1) all deposition velocities reduced to 5% of base case values (based on chamber measurements of deposition rates on glass surfaces, 12,48); 2) indoor photolysis rates computed assuming indoor photon flux in visible range is 50% of that outdoors and that ultraviolet light is further attenuated according to the transmissivity data for window glass given in Summer (50).

Table V. Source and Sink Rates (ppb h^{-1}) in Scott Gallery for Selected Species and Simulations: Average for November 4 and 5, 1984

Simulation:		Base Case		HC Source		NOx Source		Glass-Walled Bldg.	
Species	Process	Source	Sink	Source	Sink	Source	Sink	Source	Sink
NO	Ventilation	17.6	15.0	17.6	8.6	17.6	36.2	17.6	16.6
	Chemical Rxn	1.6	5.7	1.4	11.8	3.4	24.1	129	131
	Emission	0		0		38		0	
	Wall Loss		0		0		0		0
NO2	Ventilation	69	58	69	54	69	99	69	67
	Chemical Rxn	172	172	666	666	154	136	418	418
	Emission	0		0		38		0	
	Wall Loss		12		13		19		1
O3	Ventilation	58	29	58	20	58	21	58	65
	Chemical Rxn	2	8	1	25	3	23	131	123
	Emission	0		0		0		0	
	Wall Loss		23		15		17		3
HNO2	Ventilation	0.029	0.025	0.029	0.064	0.029	0.046	0.029	0.134
	Chemical Rxn	0.051	0.0001	0.161	0.0004	0.104	0.0003	0.175	0.049
	Emission	0		0		0		0	
	Wall Loss		0.055		0.125		0.086		0.019
HNO3	Ventilation	5.8	2.6	5.8	2.4	5.8	2.7	5.8	7.4
	Chemical Rxn	0.8	0	0.4	0	1.1	0	2.4	0
	Emission	0		0		0		0	
	Wall Loss		4.1		3.8		4.3		0.8
NO3	Ventilation	0.007	0.008	0.007	0.004	0.007	0.005	0.007	0.007
	Chemical Rxn	29.6	29.6	12.8	12.8	24.7	24.7	43.1	43.1
	Emission	0		0		0		0	
	Wall Loss		0.013		0.007		0.009		0.001
N2O5	Ventilation	0.4	0.5	0.4	0.2	0.4	0.4	0.4	0.5
	Chemical Rxn	29.1	28.1	12.2	12.1	23.8	23.1	38.8	38.6
	Emission	0		0		0		0	
	Wall Loss		0.8		0.4		0.7		0.1
PAN	Ventilation	2.9	1.6	2.9	1.7	2.9	1.6	2.9	3.4
	Chemical Rxn	0.8	0.8	0.9	0.8	0.8	0.8	2.6	1.9
	Emission	0		0		0		0	
	Wall Loss		1.3		1.3		1.3		0.1
HCHO	Ventilation	14.3	13.1	14.3	23.9	14.3	21.2	14.3	18.1
	Chemical Rxn	1.0	0.03	13.7	0.06	1.1	0.1	4.3	0.5
	Emission	0		0		8.9		0	
	Wall Loss		2.2		4.0		3.1		0.2
RCHO	Ventilation	12.8	12.0	12.8	25.6	12.8	12.7	12.8	20.6
	Chemical Rxn	1.3	0.05	17.5	0.1	2.0	0.1	8.8	0.9
	Emission	0		0		0		0	
	Wall Loss		2.0		4.5		2.1		0.2
H2O2	Ventilation	2.9	1.2	2.9	2.0	2.9	1.1	2.9	2.9
	Chemical Rxn	0.1	0.0001	2.2	0.0002	0.1	0.0001	0.2	0.003
	Emission	0		0		0		0	
	Wall Loss		1.9		3.1		1.8		0.2

Table VI. Species Concentrations (ppb) in Scott Gallery: Average for November 4 and 5, 1984

Species	Outdoor: Meas/Sim[a]	Indoor: Measured	Indoor Simulations: Base Case	Low NO_2 WL	No Chem	Multichamber[b]	HC Source	NOx Source	Glass-Walled
NO	31.8	32.3	27.2	27.5	30.7	27.2	15.2	38.1	26.0
NO2	59.8 [c]	52.4 [c]	45.9	61.6	45.0	46.5	48.5	70.4	61.0
O3	31.2	14.0	15.1	14.9	16.8	15.5	9.8	11.1	34.1
HNO2	0.063		0.018	0.018	0.007	0.019	0.041	0.028	0.124
HNO3	3.12		1.35	1.36	1.17	1.43	1.25	1.39	4.96
HNO4	0.343		0.176	0.181	0.133	0.184	0.646	0.135	0.304
NO3	0.0035		0.0042	0.0041	0.0014	0.0044	0.0022	0.0029	0.0046
N2O5	0.181		0.258	0.285	0.072	0.277	0.110	0.211	0.350
PAN	1.56		0.86	0.86	0.85	0.89	0.87	0.85	1.96
RNO4	0.87		0.44	0.44	0.34	0.47	2.21	0.34	0.78
RONO	0.0		0.00007	0.00006	0.0	0.00007	0.00205	0.00043	0.00107
HCHO	13.2		10.3	10.3	9.8	10.4	18.3	14.5	15.1
RCHO	11.7		9.5	9.5	8.8	9.6	21.0	9.8	16.3
HO2	0.0151		0.0079	0.0072	0.0060	0.0082	0.0400	0.0049	0.0123
H2O2	1.56		0.61	0.60	0.59	0.64	1.02	0.59	1.69
O	1.31 E-06		6.21 E-09	6.92 E-09	0.0	6.24 E-09	5.10 E-09	12.0 E-09	4.62 E-07
OH	2.80 E-03		0.22 E-05	0.21 E-05	0.0	0.23 E-05	0.22 E-05	0.40 E-05	2.41 E-05
RCO3	0.00042		0.00017	0.00015	0.00016	0.00018	0.00030	0.00011	0.00043
RO	6.03 E-07		0.37 E-07	0.35 E-07	0.0	0.38 E-07	4.62 E-07	1.08 E-07	5.10 E-07
RO2	0.0146		0.0071	0.0063	0.0058	0.0074	0.0584	0.0044	0.0104

[a] Outdoor average concentrations for species not listed: ALK - 241 ppb, ARO - 63 ppb, CO - 3.04 ppm, C2H4 - 22 ppb, OLE - 15 ppb.

[b] Volume-weighted average for four chambers.

[c] Quantitative interference from HNO3 and PAN assumed and subtracted from measured NOx-NO. For indoor value, results from base case simulation used.

Figure Captions

Figure 1. Schematic representation of the ventilation components of the multichamber indoor air quality model.

Figure 2. Floor plan of the west wing of the Virginia Scott Steele Gallery, San Marino, California. Daytime (nighttime) ventilation flow rates are given in units of $m^3\ min^{-1}$. Air sampling locations for the validation experiment are indicated by "x".

Figure 3. Comparison of modeled and measured ozone concentrations for a two-day period.

Figure 4. Comparison of modeled and measured concentrations of a) nitric oxide, b) nitrogen dioxide (NO_2*, measured as NO_x-NO), and c) total oxides of nitrogen for a two-day period. In the case of nitric oxide, the "base case" and "low (NO_2) wall loss" simulations produce essentially equivalent results.

Figure 5. Average measured and modeled pollutant concentrations for the Scott Gallery, November 4-5, 1984.

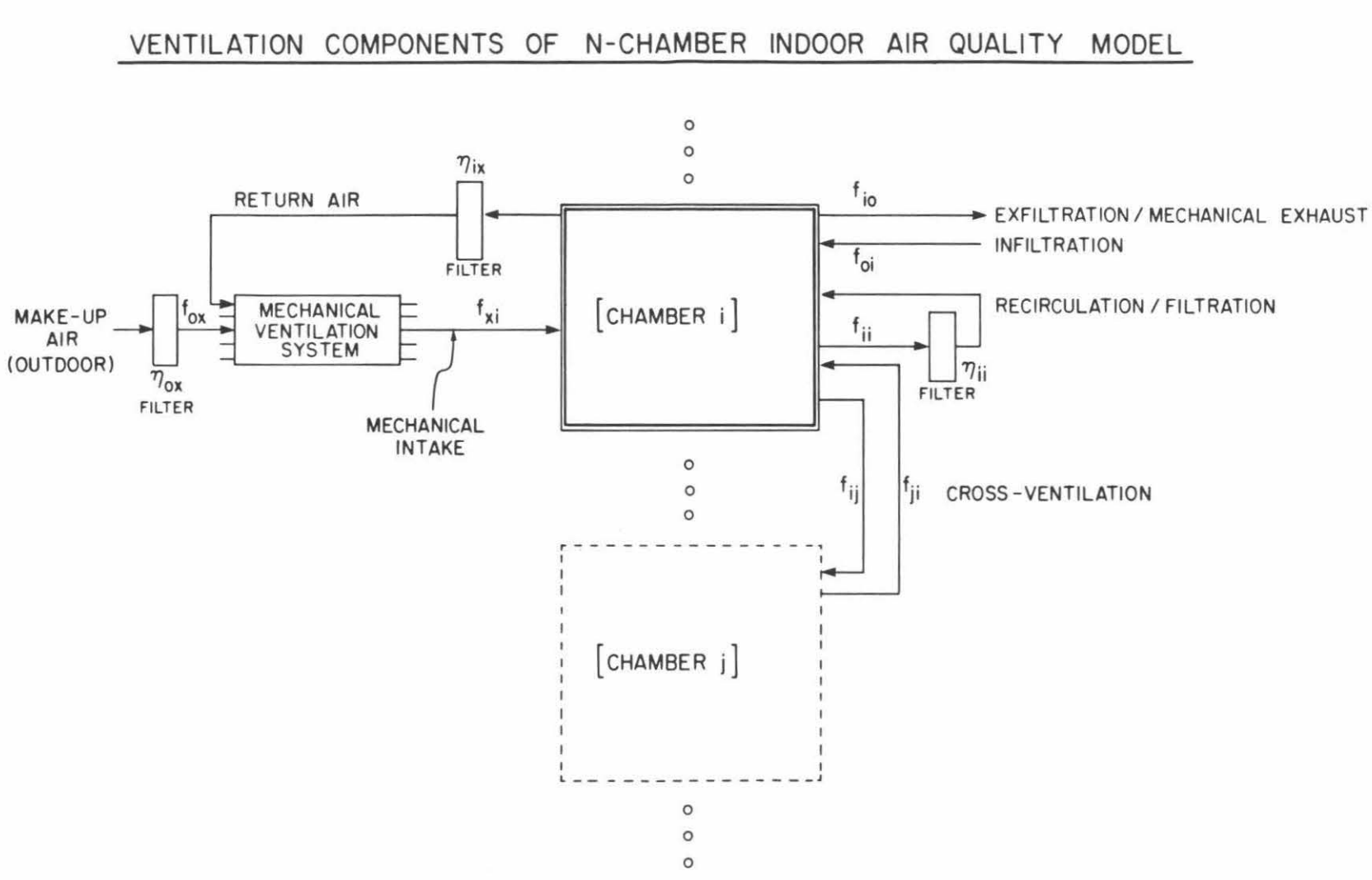
VENTILATION COMPONENTS OF N-CHAMBER INDOOR AIR QUALITY MODEL
RETURN AIR
η_{ix}
FILTER
f_{io}
EXFILTRATION / MECHANICAL EXHAUST
INFILTRATION
f_{oi}
MAKE-UP AIR (OUTDOOR)
f_{ox}
MECHANICAL VENTILATION SYSTEM
f_{xi}
[CHAMBER i]
RECIRCULATION / FILTRATION
f_{ii}
η_{ii}
FILTER
η_{ox}
FILTER
MECHANICAL INTAKE
f_{ij}
f_{ji}
CROSS-VENTILATION
[CHAMBER j]

Figure 1.

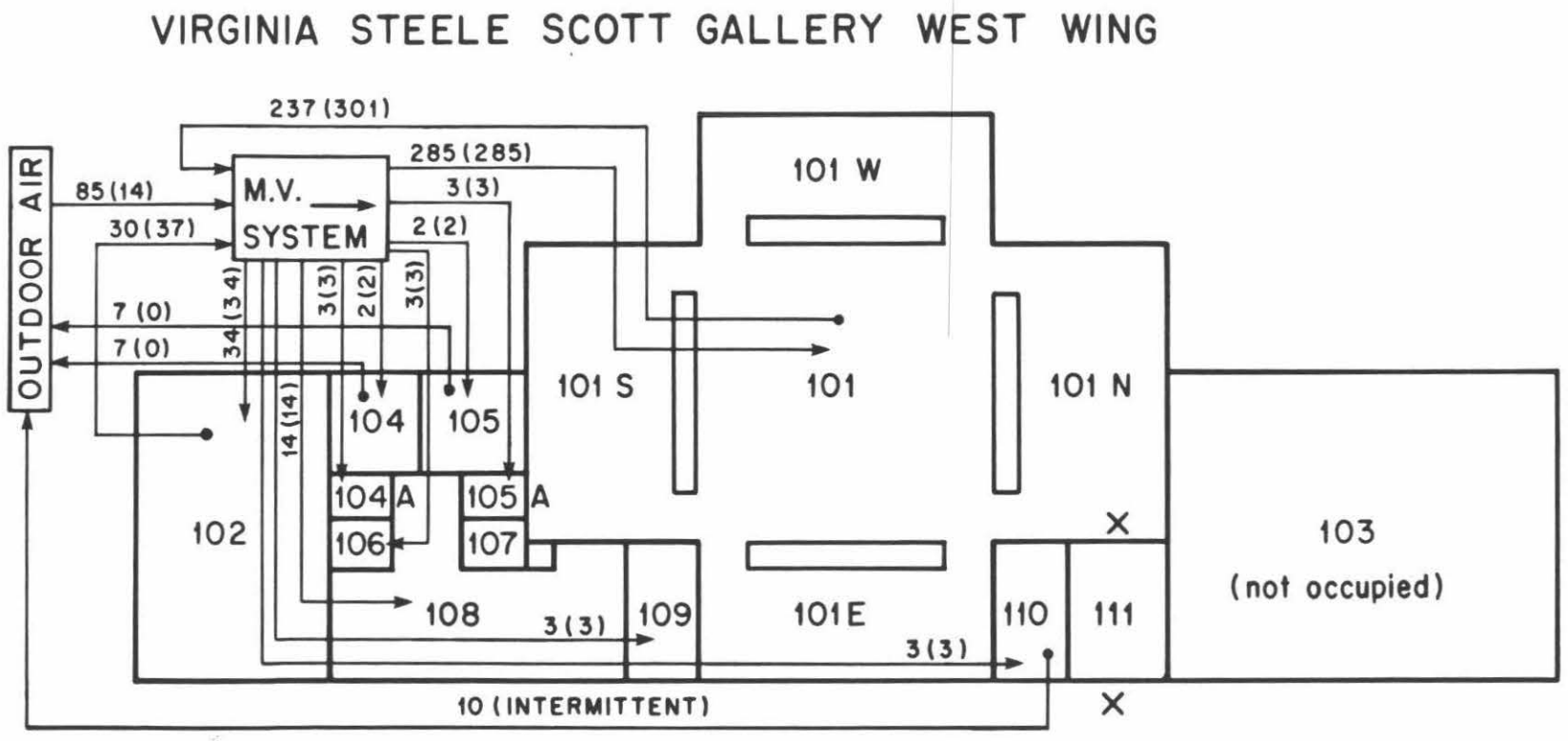
VIRGINIA STEELE SCOTT GALLERY WEST WING
237 (301)
285 (285)
85 (14)
M.V.
SYSTEM
3 (3)
30 (37)
2 (2)
OUTDOOR AIR
34 (34)
3 (3)
2 (2)
3 (3)
7 (0)
7 (0)
14 (14)
101 W
101 S
101
101 N
104
105
104 A
105 A
102
106
107
108
3 (3)
109
101E
110
111
103
(not occupied)
3 (3)
10 (INTERMITTENT)

Figure 2.

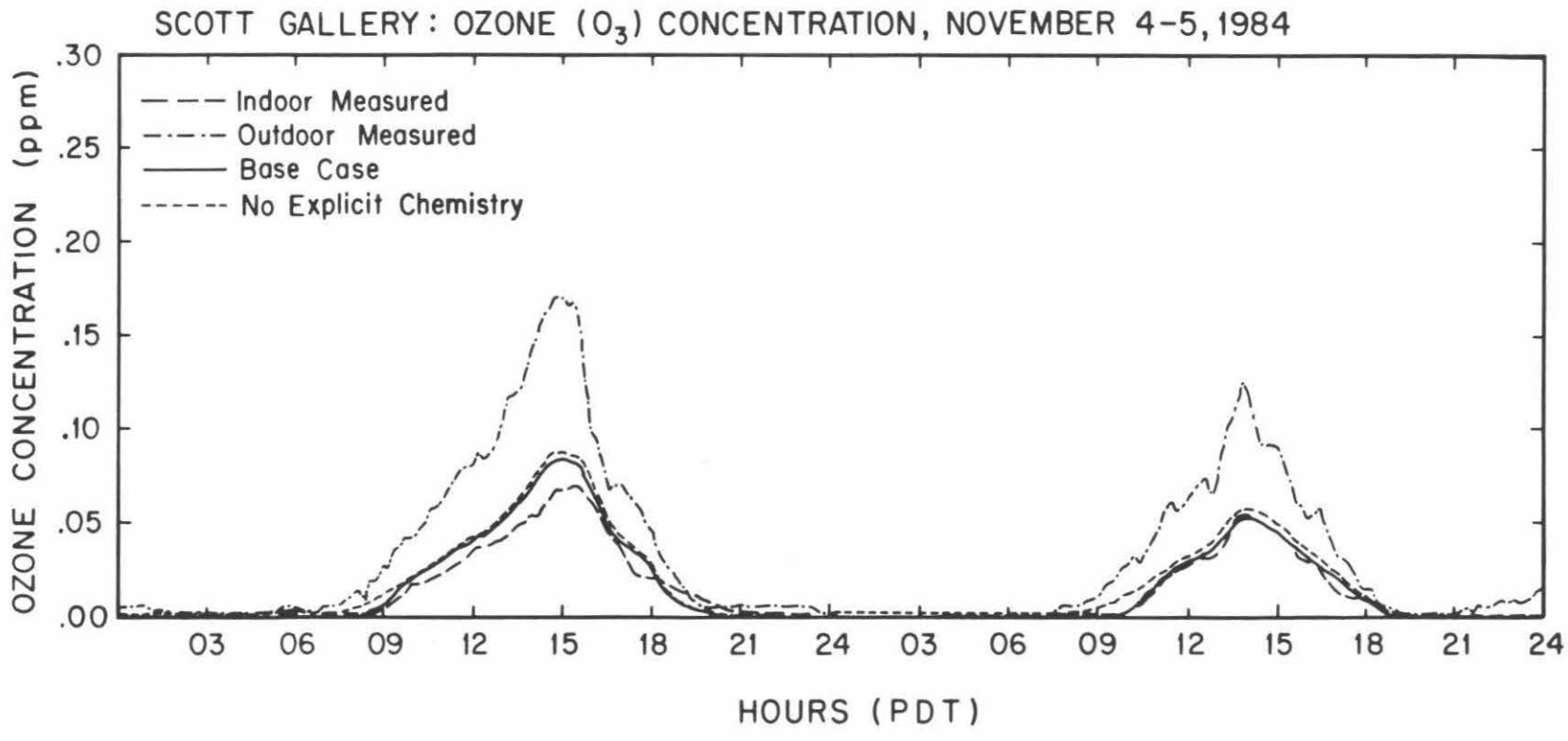
SCOTT GALLERY: OZONE (O_3) CONCENTRATION, NOVEMBER 4-5, 1984
Indoor Measured
Outdoor Measured
Base Case
No Explicit Chemistry
OZONE CONCENTRATION (ppm)
.30
.25
.20
.15
.10
.05
.00
03 06 09 12 15 18 21 24 03 06 09 12 15 18 21 24
HOURS (PDT)

Figure 3.

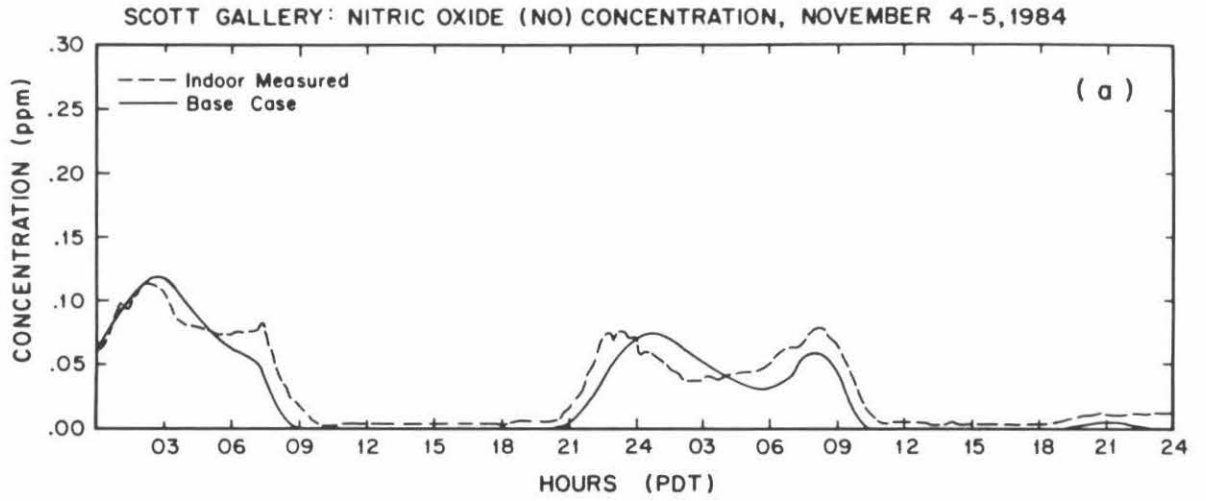
SCOTT GALLERY: NITRIC OXIDE (NO) CONCENTRATION, NOVEMBER 4-5,1984
Indoor Measured
Base Case
(a)
CONCENTRATION (ppm)
.30
.25
.20
.15
.10
.05
.00
03 06 09 12 15 18 21 24 03 06 09 12 15 18 21 24
HOURS (PDT)

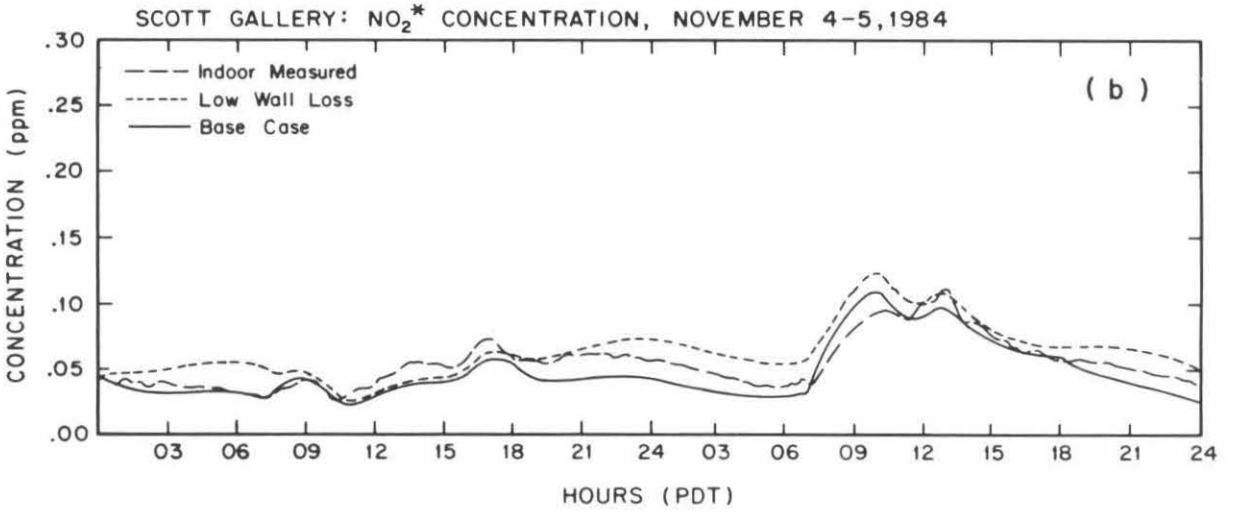
SCOTT GALLERY: NO_2^* CONCENTRATION, NOVEMBER 4-5,1984
Indoor Measured
Low Wall Loss
Base Case
(b)
CONCENTRATION (ppm)
.30
.25
.20
.15
.10
.05
.00
03 06 09 12 15 18 21 24 03 06 09 12 15 18 21 24
HOURS (PDT)

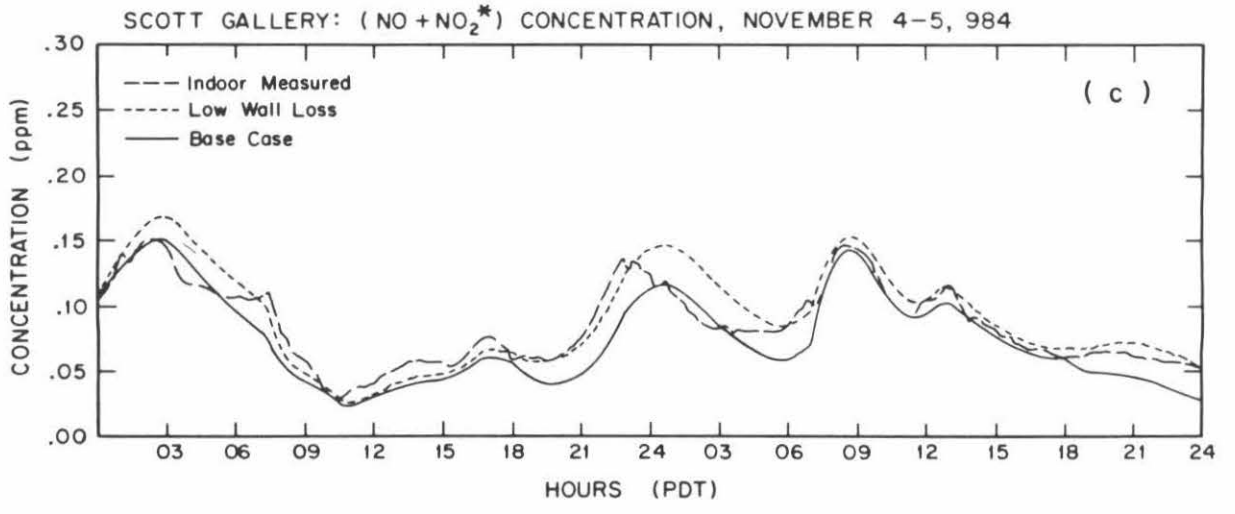
SCOTT GALLERY: (NO + NO_2^*) CONCENTRATION, NOVEMBER 4-5, 984
Indoor Measured
Low Wall Loss
Base Case
(c)
CONCENTRATION (ppm)
.30
.25
.20
.15
.10
.05
.00
03 06 09 12 15 18 21 24 03 06 09 12 15 18 21 24
HOURS (PDT)

Figure 4.

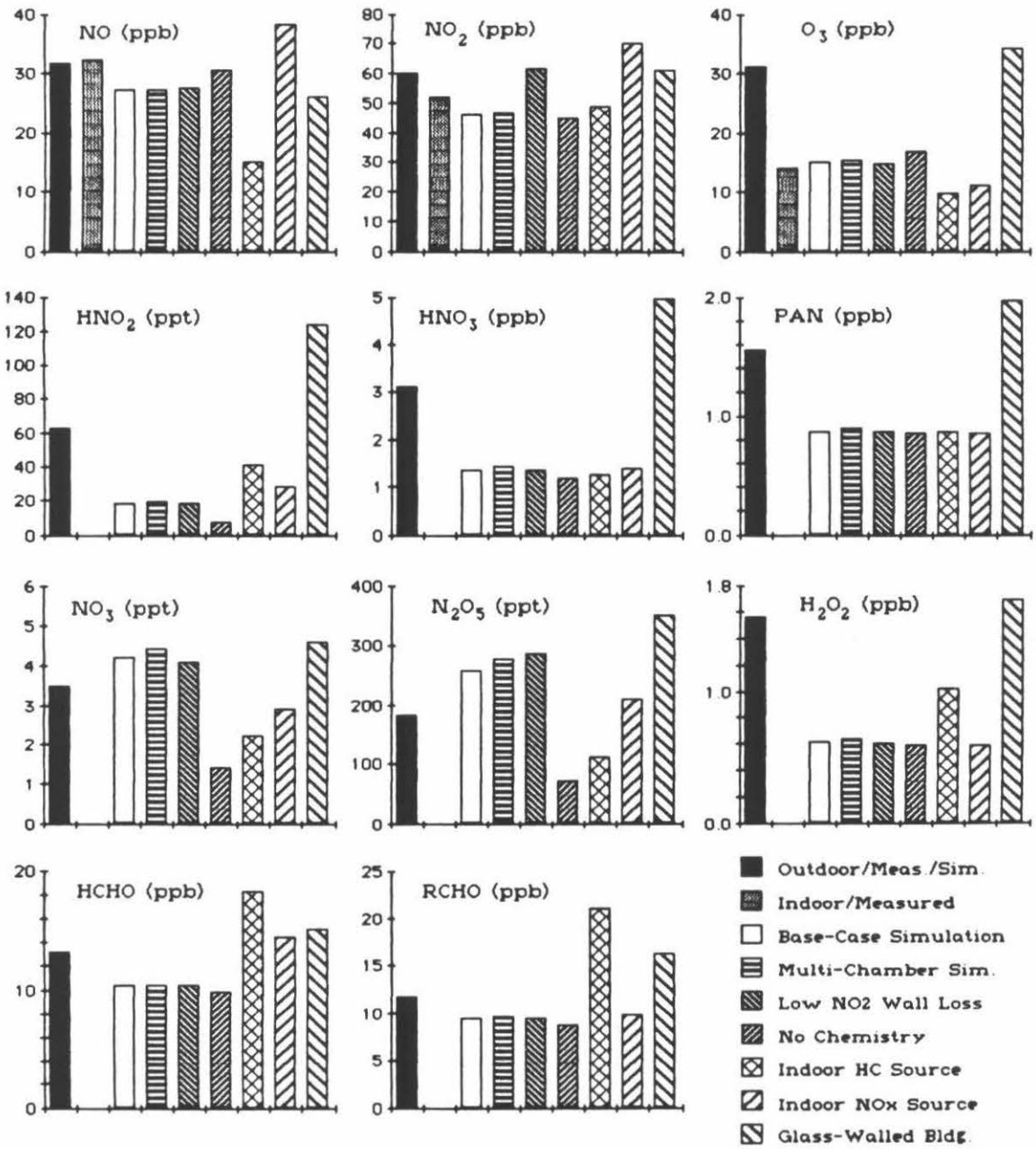
NO (ppb)
NO_2 (ppb)
O_3 (ppb)
HNO_2 (ppt)
HNO_3 (ppb)
PAN (ppb)
NO_3 (ppt)
N_2O_5 (ppt)
H_2O_2 (ppb)
HCHO (ppb)
RCHO (ppb)
Outdoor/Meas./Sim.
Indoor/Measured
Base-Case Simulation
Multi-Chamber Sim.
Low NO2 Wall Loss
No Chemistry
Indoor HC Source
Indoor NOx Source
Glass-Walled Bldg.

Figure 5.